Marine Mammal Science

MARINE MAMMAL SCIENCE, 31(3): 1193–1212 (July 2015)

DOI: 10.1111/mms.12211

Postnatal development of franciscana's (*Pontoporia blainvillei*) biosonar relevant structures with potential implications for function, life history, and bycatch

Guilherme Frainer,[1] Laboratório de Sistemática e Ecologia de Aves e Mamíferos Marinhos (LABSMAR), Departamento de Zoologia, Universidade Federal do Rio Grande do Sul (IB/UFRGS), Porto Alegre, Rio Grande do Sul, Brazil and Centro de Estudos Costeiros, Limnológicos e Marinhos (CECLIMAR/IB/UFRGS), Imbé, Rio Grande do Sul, Brazil; **Stefan Huggenberger**, Department II of Anatomy, University of Cologne, 50924 Cologne, Germany; **Ignacio Benites Moreno**, Laboratório de Sistemática e Ecologia de Aves e Mamíferos Marinhos (LABSMAR), Departamento de Zoologia, Universidade Federal do Rio Grande do Sul (IB/UFRGS), Porto Alegre, Rio Grande do Sul, Brazil and Centro de Estudos Costeiros, Limnológicos e Marinhos (CECLIMAR/IB/UFRGS), Imbé, Rio Grande do Sul, Brazil.

Abstract

Franciscana dolphins (*Pontoporia blainvillei*) are the most endangered species of the western South Atlantic Ocean. The major cause of their vulnerability is incidental bycatch in fishery gill nets. Ontogenetic changes of biosonar relevant structures in *Pontoporia* were analyzed in five specimens (one female neonate, two male neonates and two male adults) using digital imaging technology (MRI, CT) and macroscopic dissections to compare structures involved in sound production and reception. These data were compared to an ontogenetic series of 69 macerated skulls of *Pontoporia* in order to elucidate the correlation between soft tissue structures and bones of the epicranial complex and to describe the development-related changes in the mandible. Postnatal developmental shape changes of the posterior part of the right vestibular air sac followed bone formation and the melon with its right branch elongated, paralleling the flatter facial depression of adults. Minor postnatal developmental modifications were verified in the tympano-periotic complex but a shape change of the mandible was visible by a ventral deviation of the posterior part of the mandible in adults. These results reveal postnatal changes in allometry and shape of biosonar relevant structures that may be one of the causes that increase bycatch of neonate and young *Pontoporia* individuals.

Key words: franciscana dolphin, *Pontoporia blainvillei*, ontogeny, anatomic geometry, functional anatomy, echolocation, conservation.

To generate and receive sound pulses for echolocation, toothed whales (Cetartiodactyla: Odontoceti) have evolved a complex apparatus associated with the nasal tract and a unique fatty acoustic pathway at the mandibles to guide sound to the middle ears (Norris *et al.* 1961, Evans and Prescott 1962, Purves and Pilleri 1983, Cranford *et al.* 1996, Aroyan 2001). By using this sonar apparatus toothed whales are able to

[1]Corresponding author (e-mail: gui.frainer@gmail.com).

explore and hunt in different environments, such as coastal, pelagic and deep waters as well as in estuarine and river systems.

Norris *et al.* (1961) verified that a blindfolded dolphin can detect objects placed rostrodorsal of the mouth, but not below the rostrum line. Since then it has been accepted that the sound beam formation for echolocation is originated in the epicranial (nasal) complex, more specifically in the "monkey lips dorsal bursae" (MLDB) complex (Cranford *et al.* 1996, Cranford *et al.* 2008*b*). The monkey lips, or phonic lips, are valve-like structures in the soft nasal tract at the dorsal end of the nasal plugs. They produce snap-like noises in a series of events, specific for each species (Akamatsu *et al.* 2007), resulting from pneumatic actuation of the phonic lips (Cranford and Amundin 2004, Cranford *et al.* 2008*b*). These slapping events generate vibrations in two adjacent small fat bodies named dorsal bursae (Fraser and Purves 1960, Cranford *et al.* 1996), which are closely placed posterior to the caudal end of the melon. Cranford *et al.* (1996) pointed out that the left and right MLDB complexes of toothed whales (except sperm whales, *Physeter macrocephalus*) should operate simultaneously and with variable phase relationship between one another. These vibrations of the MLDB are reflected anteriorly by the skull and nasal air sacs, functioning both as acoustic mirrors. In most small odontocetes, there are four pairs of air sacs surrounding the nasal passage between the skull and the blowhole: the premaxillary air sacs, immediately dorsal to the skull and directly upon the periosteum of the premaxillae; the inferior vestibules, along the posterior edge of the nasal passages; the nasofrontal air sacs, divided into one anterior and one posterior portion and surrounding the nasal passage just dorsal to the right posterior dorsal bursa; and the superficial vestibular air sac, extending laterally from the nasal passage in a horizontal plane just dorsal to the nasal plugs (Mead 1975, Cranford *et al.* 1996). The nasal diverticulum is the most variable portion of delphinid nasal complex (Mead 1975), operating both as air reservoirs during sound production and as acoustic reflectors (as cited above) that will concentrate the sound energy into the melon (Cranford *et al.* 1996, 2008*b*). The melon is functionally important to focus the sound energy generated in the MLDB complex as it decreases the acoustic attenuation at the animal-environment interface by impedance matching (Norris and Harvey 1974, Harper *et al.* 2008, McKenna *et al.* 2012).

In toothed whales, the soft external auditory meatus is present but narrow, and its potential functional implications in hearing are unclear. There are different hypotheses on how sound is transmitted to the middle ear in these animals bypassing the external auditory meatus. A possible analogue of the mammalian outer ear can be regarded as an extended acoustic fat body around and within each dental bone in the lower jaw of toothed whales. Accordingly, the clicks produced by the epicranial complex are reflected by objects and then received *via* intramandibular fat bodies by the tympano-periotic complex and the middle ear, respectively (Bullock *et al.* 1968, Norris 1968). Whether the sound waves reach the intramandibular fat bodies through the acoustic window in the lower jaw (Norris 1968), or through an alternative hearing pathway of the gular region, as demonstrated in a single *Ziphius* specimen (Cranford *et al.* 2008*a*), is a matter of an ongoing debate.

Although the gross anatomy of sound generating and receiving structures in the toothed whale head has been well described (*e.g.*, Cranford *et al.* 1996, Cranford and Amundin 2004, Cranford *et al.* 2008*b*, Huggenberger *et al.* 2009), developmental studies are scarce (Rauschmann *et al.* 2006, Galatius *et al.* 2011, Moran *et al.* 2011, Haddad *et al.* 2012) and there are no detailed descriptions on the postnatal development of soft tissues of the head. Accordingly, herein we focus on the postnatal

development of biosonar relevant structures in one toothed whale species, the franciscana (*Pontoporia blainvillei*) whose adult nasal complex has been described in some detail in literature (Burmeister 1867, Schenkkan 1972, Cranford *et al.* 1996, Huggenberger *et al.* 2010).

In comparison to a dolphin skull, such as *Tursiops*, *Pontoporia* has a long narrow bony rostrum, with a concave ventral profile in lateral view, and exhibits the most symmetrical skull of any extant odontocetes (Ness 1967, Barnes 1985, Cranford *et al.* 1996) (Fig. 1). The small braincase with one of the smallest brains among toothed whales (Schwerdtfeger *et al.* 1984, Manger 2006) may correlate with the elongation of *Pontoporia*'s nasal complex. Huggenberger *et al.* (2010) have noted that this elongation is marked by topographical relations of the dorsal bursae with the cranial vault and melon, which is located further caudally in relation to the brain case. In odontocetes with larger brains (*e.g.*, *Tursiops*), however, the cranial vault extends dorsally and the epicranial complex is shifted in a more dorsorostral position (Huggenberger *et al.* 2010).

The presence of two anatomically distinct fatty paths from each MLDB complex to the melon (branches of melon) is a particularity in *Pontoporia* (Cranford *et al.* 1996, Huggenberger *et al.* 2010). A further particularity is *Pontoporia*'s extreme soft tissue asymmetry in the superficial area of the nasal complex, whereas the facial skull is nearly symmetrical (Schenkkan 1972, Cranford *et al.* 1996, Huggenberger *et al.* 2010). The extreme asymmetry of *Pontoporia*'s nose is characterized by a region of connective tissue found solely in the left branch of the melon and by a hyperdevelopment of the right vestibular air sac that surpasses the medial axis of the head to a point near the rostral margin of the left vestibular air sac (Schenkkan 1972, Cranford *et al.* 1996). Huggenberger *et al.* (2010) have proposed that *Pontoporia*'s epicranial complex should show marked sound emission lateralization, in which the left side generates a wider beam (because of its incomplete left branch of the melon that is not entirely covered by air sacs) while the complete elongated right branch of the melon may generate a more focused beam. However, the focusing of *Pontoporia*'s sound beam may be restricted by the small melon size, the few layers of the facial muscle (three instead of six), as well as the absence of the rostral part of the facial muscle (*musculus maxillonasolabialis pars rostralis*). Nevertheless, the functionality of the plesiomorphic

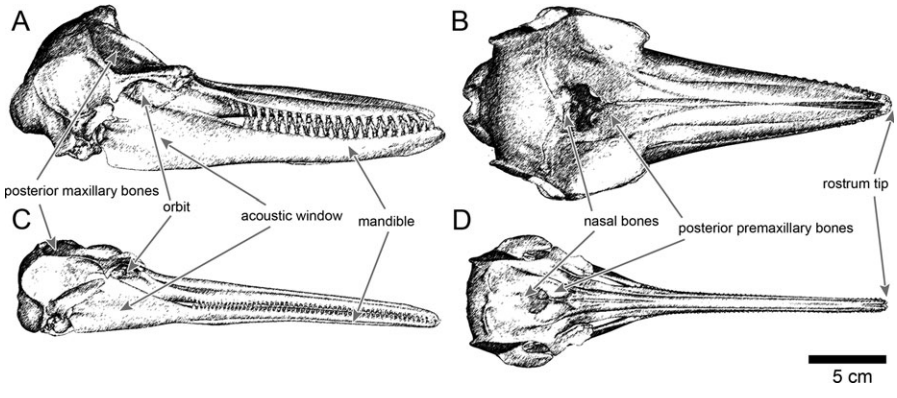

Figure 1. Illustrations after 3D reconstructions of CT data comparing the skull morphology of *Tursiops* (G1447) and *Pontoporia* (G1465) in lateral (A–C) and dorsal view (B–D), respectively.

conditions in *Pontoporia*'s nasal complex is still a matter of discussion (Cranford *et al.* 1996, Huggenberger *et al.* 2010).

This study of *Pontoporia*'s biosonar relevant structures is of general interest because *Pontoporia* is the most endangered species of the western South Atlantic Ocean (Praderi *et al.* 1989; Secchi *et al.* 2001, 2003). The major cause of their vulnerability is incidental bycatch in fishery gill nets (Secchi *et al.* 1997, 2003). Read *et al.* (2003) have reported several factors that may affect the entanglement of odontocetes in fishing nets, including behavioral peculiarities and failure of net detection by echolocation. Modified composition of net materials in order to increase acoustic reflectivity has reduced the mortality in some toothed whale species (Kraus *et al.* 1997, Bordino *et al.* 2002). However, this mitigation effort has not had positive effects on the number of bycatches of *Pontoporia* (Bordino *et al.* 2013).

Intriguingly, more than half (51%) of bycaught *Pontoporia* individuals are young (<3 yr old; Moreno *et al.* 1997, Ramos *et al.* 2000). However, whether or not this preponderance for young individuals can be attributed to immature development of the echolocation systems, as others have hypothesized for delphinids (Gardner *et al.* 2007), still remains a matter of speculation. Accordingly, the present study focuses on the ontogenetic changes of the biosonar relevant structures (nasal complex and hearing apparatus) in the head of *Pontoporia* in postnatal stages, which are the most critical stages regarding bycatch threats.

Material and Methods

The description of biosonar relevant structures of *Pontoporia blainvillei* was based mainly on (1) magnetic resonance imaging (MRI) of one male neonate (6.43 mm slice thickness, 0.469 mm pixel edge length) and one male adult (7.99 mm slice thickness, 0.586 mm pixel edge length); (2) transverse computed tomography scans (CT) of another male neonate (1 mm slice thickness, 0.277 mm pixel edge length), and the same adult head (1 mm slice thickness, 0.586 mm pixel edge length); (3) macroscopical dissections (DS) of one male adult, two neonates, and one male subadult (Table 1).

All of the examined fresh material (carcass condition: code 2; see Geraci and Lounsbury 1993) was obtained from incidentally caught individuals by fishery activity and

Table 1. List of soft material examined.

Institution[a]	ID number	Age	Body length (cm)	Sex	Fixation	Method applied
GEMARS	1441	Adult	155	M	Frozen	DS
GEMARS	1465	Adult	138.1	M	Frozen	CT, MRI
GEMARS	1440	Subadult	124	M	Frozen	DS
GEMARS	1417	Neonate	84	M	Frozen	DS
GEMARS	1472	Neonate	75.5	F	Frozen/formalin	MRI/ DS
GEMM	220	Neonate	68.9	M	Frozen	CT

Note: Methods applied: CT, computer assisted tomography; DS, macroscopical dissection; MRI, magnetic resonance imaging.

[a]GEMARS, Grupo de Estudos de Mamíferos Aquáticos do Rio Grande do Sul, Brazil; GEMM, Grupo de Estudos de Mamíferos Marinhos da Região dos Lagos, Brazil.

belong to the scientific collection of the Grupo de Estudos de Mamíferos Aquáticos do Rio Grande do Sul (GEMARS), except for one male neonate from the scientific collection of the Grupo de Estudos de Mamíferos Marinhos da Região dos Lagos (GEMM) (Table 1). The MRI scans of the thawed specimens and CT scans were performed in all three planes defined by Huggenberger *et al.* (2010). The anatomical topography was described using InVesalius imaging processing software (de Moraes *et al.* 2012), including measurements of distances, angles, volume, and density values (Hounsfield units, HU). HUs express a calibrated measure of electron density within each "voxel" in a three-dimensional image (McKenna *et al.* 2012) and are adjusted so that −1,024 HU is the attenuation of air while 0 HU is the attenuation of water (Robb 1999). HUs are correlated with density properties (McKenna *et al.* 2012) and the volume values are directly comparable in DICOM images format (McKenna *et al.* 2007). The reconstruction of single structures comprises the basic components of the sound production and reception apparatus in *P. blainvillei* that were determined using the segmentation technique described by Cranford *et al.* (2008*b*), that is, images were analyzed and edited voxel by voxel on the three planes accomplished with a threshold assistance tool. The dissections followed Schenkkan (1972) in that ". . .the different layers of muscles connected with the blowhole region were dissected layer by layer, keeping adjacent structures intact as much as possible." In addition, histological sections (HIS) stained with Masson technique (Prophet *et al.* 1992) were performed in the rostral part of the epicranial complex in a neonate specimen (GEMARS 1472).

For comparison, 69 skulls, including 42 males (BL, body length mean: 115.51 cm, SD: 24.718; CBL, condylobasal length mean: 32.47 cm, SD: 4.419) and 27 females (BL mean: 135.17 cm, SD: 21.823; CBL mean: 35.27 cm, SD: 5.850), were examined in order that ontogenetic changes of facial bones (*i.e.*, maxillae and nasal bones) as well as mandible, including the form and closure of the mandibular alveoli by the interalveolar septa, were analyzed. Standard length and width measurements of both tympanic and periotic bones (Kasuya 1973) were taken to compare them to the skull (CBL) and ear bone of the CT scanned specimens. Terminology follows Cranford *et al.* (1996) and Mead and Fordyce (2009).

Results

Although we were able to describe the main structures of the biosonar system (epicranial complex and sound perception apparatus) in both calf and adult specimens, some structures of the calf's skull do not appear in the CT image reconstructions because of the low density of these parts and the low CT scan acuity, resulting in undistinguishable areas (Oelschläger *et al.* 2008). The following results focus on comparison of the biosonar relevant structures in neonate and adult *Pontoporia* specimens.

Development of the Sound Production Apparatus

Monkey lips—In general, at the dorsal end of the paired nasal passages, the monkey lips were visible as a low horizontal ridge on the anterior and posterior walls of each nasal passage. Thus, the lips stood perpendicular to the air stream. The horizontal ridges were characterized by a series of small wrinkles oriented parallel to the air stream (Fig. 2). The monkey lips in neonate specimens exhibited the same wrinkles

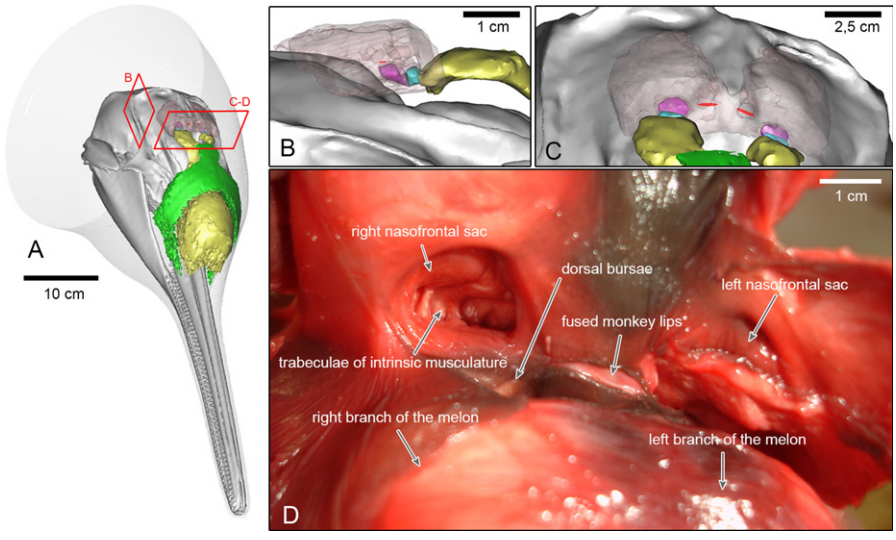

Figure 2. 3D reconstructions of the main structures involved in sound production (melon, yellow; anterior bursa, cyan; posterior bursa, magenta; connective tissue theca, green; tendinous fibres of *m. maxillonasolabialis*, pink and low translucent) of a CT scanned adult *Pontoporia* (GEMARS 1465, CBL: 38.7 cm) incidentally captured in fishery activities. The skin is shown in gray and the pair of monkey lips is illustrated in red. A dorsofrontal side view of the complete head (A) lateral, (B), and frontal (C) detail views. (D) Subadult male (GEMARS 1440) dissection showing the main structures involved in sound production. On this frontal view, the dense part of *musculus maxilonasolabialis* was elevated to expose the nasofrontal air sacs (with the trabeculae of the intrinsic musculature forming internal invaginations of diverticulum walls), dorsal bursa, and *a single case of fused posterior monkey lips exhibited by this specimen, see main text.

and size proportions as the monkey lips in the adults. One male subadult (GEMARS 1440) revealed a medial fusion of both posterior monkey lips (the posterior dorsal bursae were not fused) (Fig. 2D) and this may potentially represent a random condition of the monkey lips. Interestingly, the small wrinkles were continuous along this wide lip.

Dorsal bursae—These two different pairs of ellipsoid fat bodies, the posterior (PB) and the anterior (AB) dorsal bursae (Figs. 2–4), were situated perpendicularly in relation to the body axis, whose largest diameter was aligned approximately in a mediolateral axis. The PBs were located at the posterior wall of each nasal passage, closely adjacent to the posterior monkey lips, and below the nasofrontal sacs (see below; Figs. 2–4). The ABs were placed on the anterior wall of each nasal passage adjacent to the anterior monkey lips. In the CT scanned neonate specimen, the right PB (axial length 3.2 mm and width 5.15 mm) was larger than the left PB (axial length 3.74 mm and width 4.77 mm). The same was found in the adult specimen (right PB axial length 4.25 mm and width 6.91 mm, left PB axial length 4.28 mm and width 6.41 mm). This asymmetry was reflected also by the PB volume of the neonate (right PB 35.76 mm^3, left PB 31.53 mm^3) and the adult (right PB 70.38 mm^3, left PB 54.93 mm^3). We could distinguish the limits of the ABs from the posterior branch of the melon (see below) in both specimens, although the male neonate

showed low differentiation between AB and posterior branches of the melon (Fig. 3, 4). The ABs and PBs were similar in shape (*i.e.*, width always larger than the axial length). The neonate's right AB (axial length 2.25 mm and width 3.08 mm) was larger than its left AB (axial length 1.53 mm and width 2.73 mm). The same was found in the adult specimen (right AB axial length 3.28 mm and width 6.08 mm, left AB axial length 3.92 mm and width 5.31 mm). In relation to CBL, the AB exhibited smaller volumetric proportions (right AB 26.53%, and left AB 17.23%) than the PB (right PB 50.81%, and left PB 57.41%).

The posterior dorsal bursae were aligned dorsoventrally with the anterior edge of the nasal bones in both the neonate and the adult (Fig. 3). In addition, the difference between the elevation angles (determined as the angle between the axis of the skull and the line that passes through the tip of the melon to the nasal passage between the dorsal bursae; Huggenberger *et al.* 2010) of the dorsal bursae of a neonate (18.9°) and an adult (16.9°) was 2° (Fig. 3C, D).

Melon—As in delphinids, the anterior portion of the epicranial complex of *Pontoporia* is composed of a prominent fat body (melon) associated with dense connective tissue and rostral muscles (Fig. 5). *Pontoporia*'s melon is characterized by a considerable directional asymmetry because the right branch of the melon, or melon terminus, connects to the right anterior dorsal bursae. The left branch of the melon, in contrast, consists only of an independent triangular fat body rostral of the left anterior dorsal bursa. Anteriorly, the right branch of the melon melon terminus meets the main body of the melon just rostral of the prominent premaxillary eminences. The ventral surface of the melon extends ventorostrally accompanying the premaxillary and maxillary curvature of the forehead surface (Fig. 3C, D). Accordingly, the main body of the melon was symmetrical in the center of the beak-fluke axis (Fig. 3A, B).

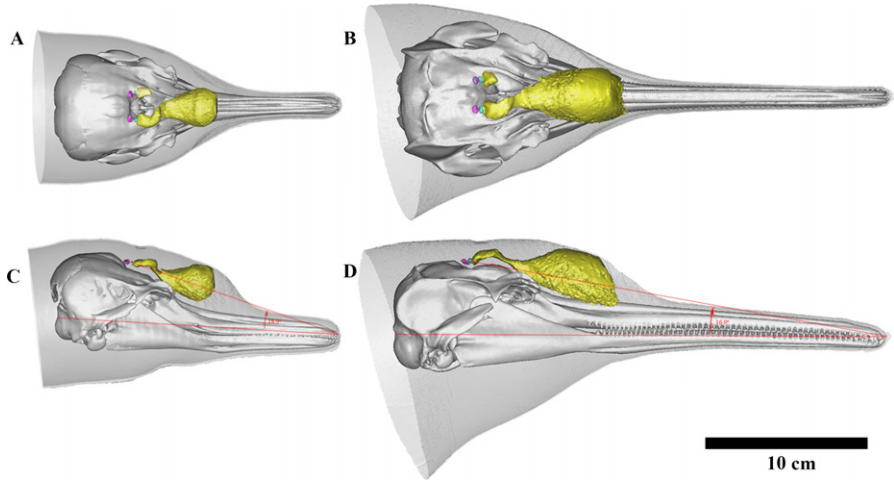

Figure 3. Dorsal (A, B) and right lateral (C, D) views of neonate (CBL: 19.4 cm) and adult (CBL: 38.7 cm) foreheads of *Pontoporia*, showing the skull and lower jaw (white), the skin (gray) and the main structures included in sound production apparatus: melon, yellow; anterior dorsal bursa, cyan; posterior dorsal bursa, magenta. The red lines in C and D represent the elevation angle of the dorsal bursae position (see Results).

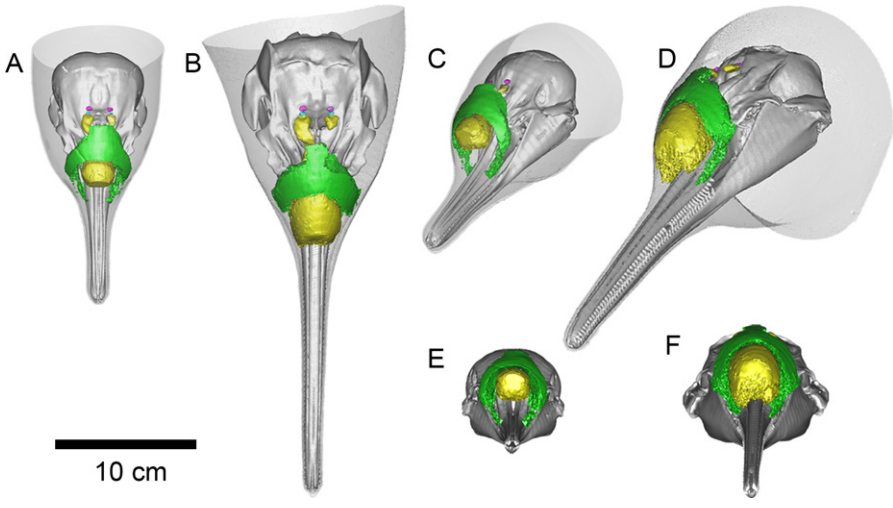

Figure 4. This reconstruction shows the sound production apparatus (melon, yellow; anterior dorsal bursa, cyan; posterior dorsal bursa, magenta) of neonate (CBL: 19.4 cm) and adult (CBL: 38.7 cm) *Pontoporia* specimens and the connective tissue theca (Ctt), green, in three different angles of view: A–B, dorsal; C–D, diagonal; E–F, frontal (head contour omitted). Note the gap formed by different tissue properties (densities) between the melon and the Ctt in neonate specimen.

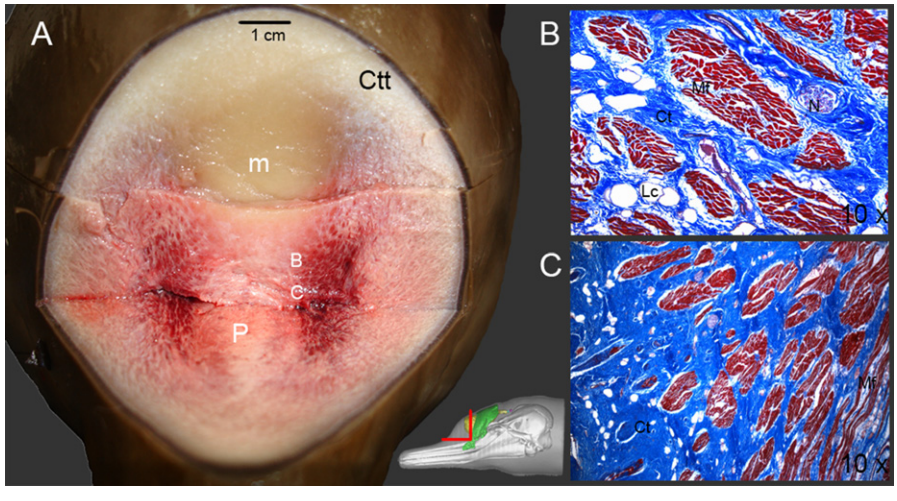

Figure 5. A. Frontal section of a neonate female *Pontoporia* (CBL: 18.7 cm) showing the rostral musculature below the melon (m). Ctt = connective tissue theca, Pm = premaxilla. B. Histological section of the rostral musculature associated with fat and connective tissues immediately ventral to the melon of a neonate *Pontoporia*. Mf = muscle fibers, Ct = connective tissue, Lc = lipidic cells, N = nerve bundle. C. Histological section of rostral musculature close to the rostral bones of a neonate *Pontoporia*. The lipid cells were scarce and the main structures are connective tissue (Ct), as well as longitudinal and transversal muscle fibers (Mf).

The postnatal developmental changes of the left branch of melon were not as remarkable as the anterior elongation and the expansion of the main melon with its right branch. The right melon terminus (right branch) of neonates exhibited a round, more accentuated lateral curvature in comparison to adult specimens (Fig. 3A, B). In neonates, the connection of the right melon terminus to the main body of the melon turned anteriorly in a steeper angle than in adults. This angle paralleled the surface of the facial depression, which was deeper in neonates (Fig. 3C).

Although no rostral musculature has been described for *Pontoporia* (Huggenberger *et al.* 2010), our histological analysis of the anterior forehead showed a series of longitudinal and transversal muscle fibers of the *musculus maxillonasolabialis pars rostralis* immediately ventral and ventrolateral to the melon (Fig. 5). This condition was found in all of the dissected neonate specimens ($n = 3$), contrasting with the adult specimens in which the anteriormost portion of the melon was attached to the premaxillary and maxillary bones (Fig. 3D) without connecting to the rostral musculature. Accordingly, in neonate specimens, the melon did not touch the rostrum bones (Fig. 3C).

In contrast to the modifications of the melon's shape, the epicranial complex length (distance from the rostroventral tip of melon to the nasal passage between the dorsal bursae; Huggenberger *et al.* 2010) of neonate (65.05 mm) and adult (126.72 mm) specimens maintains basically the same proportions in relation to CBL: 33.5% and 32.7%, respectively. However, the two melon branches developed differently in terms of length and width. The neonate specimen's melon with its right branch was 60.17 mm long while the left branch of melon was 10.08 mm long. The adult specimen's melon and its right branch was 112.84 mm long (90.38 mm + 22.46 mm, respectively) while the left branch of melon was 13.44 mm long. Therefore, the neonate's left branch of melon was 75% of the axial length of the adult's left branch of melon. On the other hand, the length of the neonate's melon with its right branch (43.43 mm + 16.74 mm, respectively) was 53.3% of the adult's structure and the neonate's melon volume with the right branch was 19.64% of the same structure in the adult. The volume of the left branch of melon (257.52 mm^3) was 53.6% of the adult's left branch of melon (480.3 mm^3). The width of the right branch of the melon (neonate: 8.78 mm; adult: 12.94 mm) was larger than the left (neonate: 7.71 mm; adult: 12.63 mm). In general, these data have shown that the melon and its branches change their shapes and the length and volume growth was not proportional.

Premaxillary air sacs—These are protrusions of the nasal tract disposed just ventral to the melon terminus on both sides on the premaxilla surface. When compared to the other paired diverticula (nasofrontal and vestibular air sacs, see below), the premaxillary sacs are nearly symmetric and they are the smallest diverticulae in *Pontoporia* (except *Pontoporia*'s left nasofrontal sac). We have found no clear changes in shape and relative size of this structure in neonates compared to adults (not shown in the figures) from our dissections.

Nasofrontal air sac—These are invaginations in a tough (dense) connective tissue attached to the maxillonasolabialis muscle, located in a level superficial to the MLDB complex (Fig. 2). The right nasofrontal sac was always bigger than the left one, and showed a series of invaginations of the lateral wall of this diverticulum containing trabeculae of the intrinsic musculature.

Vestibular air sacs (VS)—The adult right VS is delimited posteriorly by the caudal ascendant process of the maxilla and anteriorly by the line that passes transversally across both preorbital processes of the frontal bone. Moreover, the rostral part of the right VS runs to the head's left side. In our dissections, it was possible to identify

internal invaginations forming small outpockets at the anterodorsal profile of the right VS in the adult specimens (Fig. 6). This feature was present in the dissected subadult specimen, but not developed in the dissected neonate specimens, in which the anterodorsal edge was convex and smooth. The lateral profile of the VS also displayed internal invaginations in all specimens although they were less developed in newborn calves when compared to adults. The anterior edge of the VS changes from a convex shape in neonates to a slight concavity to the left-hand side in adults (Fig. 6). Also, the caudal portion of the right VS changes both its form and arrangement in the epicranial complex during postnatal ontogeny. In neonate specimens, the caudal edge of the right VS is round and does not reach the level of the supraoccipital crest. The caudal profile of the right VS in adults parallels the posterior limits of the nuchal crest and is thus close to the lateral edge of the right maxillary crest. When comparing the osteological material, it was obvious that the caudal portion of the maxillary

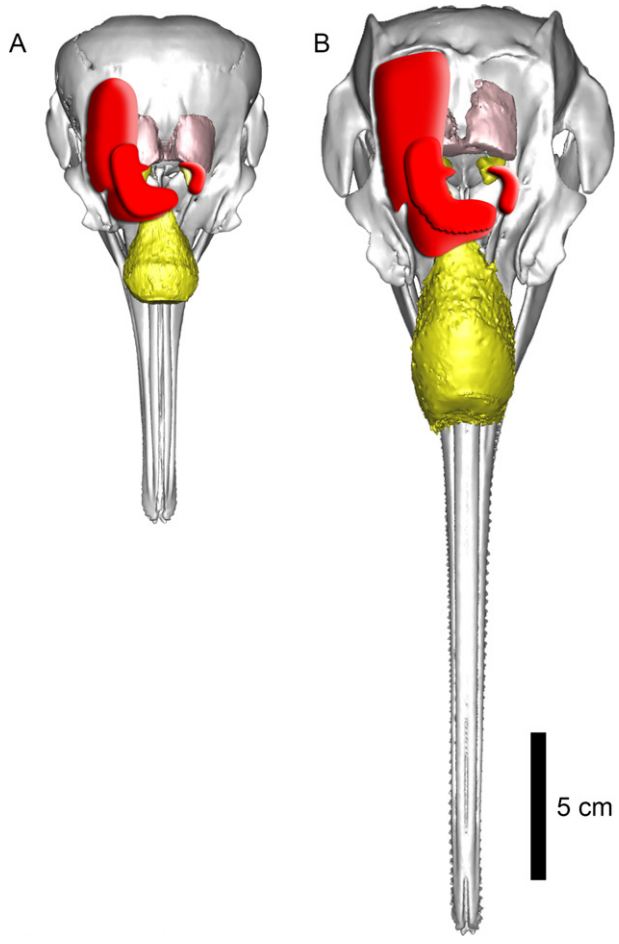

Figure 6. Dorsal views of the *Pontoporia* epicranial complex. Right and left vestibular air sacs (VS) illustrated in red. (melon, yellow; dense part of *m. maxillonasolabialis*, pink) A. Neonate specimen configuration. B. Adult and subadult specimens configuration.

bone had close similarity to the shape development of the right VS (Fig. 7). In neonates of both sexes, the less developed nuchal crest showed a round profile and, in adults, it adjoined closely the maxillary bone together with frontal, supraoccipital, and interparietal bones to form a distinct nuchal crest (n = 10, CBL range: 22.31–27.59 cm) (Fig. 7A, B). When the developing maxillary bone reaches this crest, the profile becomes more straight and parallel to the mediolateral axis (n = 57, CBL range: 27.68–41.39 cm) (Fig. 7C–F). In addition, the lateral profile of the ascendant process of the maxilla, just posterior to the orbit region, develops from a convex to a concave shape (Fig. 7). The posterior part of the premaxillary bone grows dorsally to form premaxillary eminences. These eminences expand anteriorly in which their dorsalmost surface becomes rounded in lateral view, surpassing the line that horizontally crosses the anterior insertion of the nasal bones (n = 48, CBL range:27.68–42.27 cm) (Fig. 8C, D).

Development of Sound Perception Apparatus

Mandible—In *Pontoporia*, the mandible displays allometric changes mainly regarding its alignment with the skull. In young specimens, the ventral profile in lateral

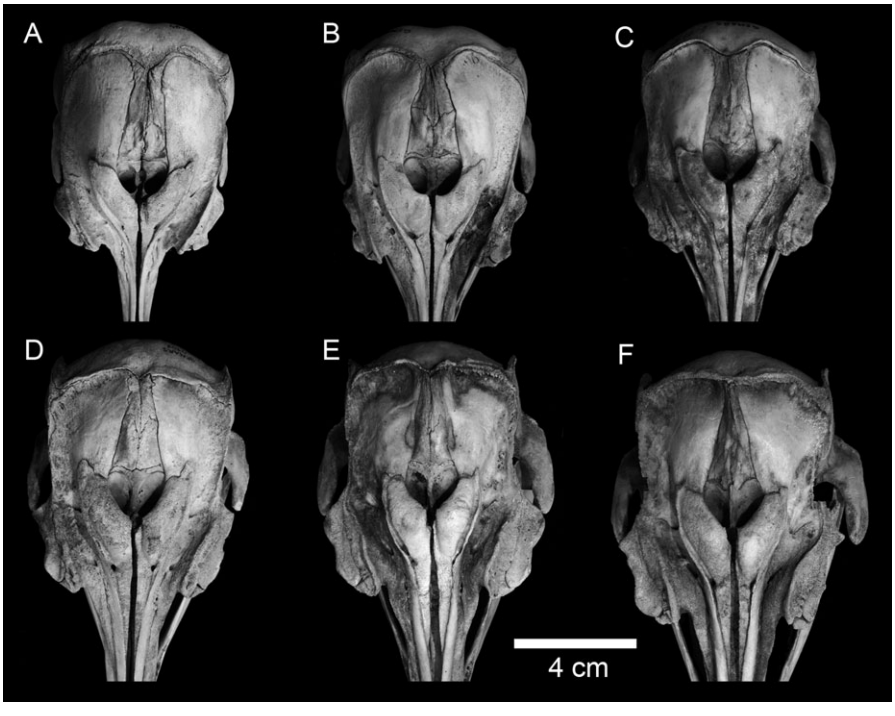

Figure 7. Dorsal views of six *Pontoporia* skulls of different developmental stages including a neonate (A), a calf (B), two subadult (C, D) and two adults (E, F) showing the modifications of the ascendant (caudal) part of the maxillary bone and the shape of the nuchal crest. A. GEMARS 777, CBL: 22.5 cm. B. GEMARS 533, CBL: 27.6 cm. C. GEMARS 1195, CBL: 30.2 cm. D. GEMARS 452, CBL: 32.7 cm. E. GEMARS 627, CBL: 41.4 cm. F. GEMARS 420, CBL: 41.5 cm.

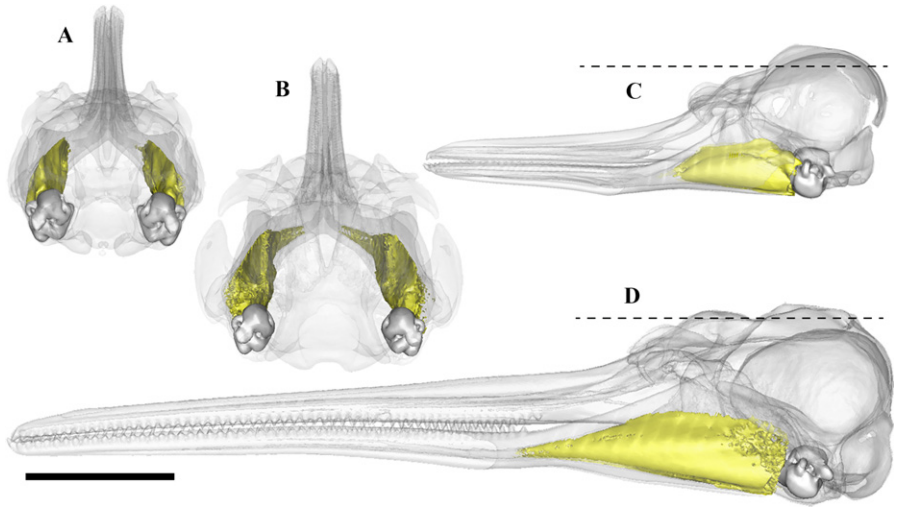

Figure 8. Posterior (A, B) and left lateral (C, D) views of the sound perception apparatus of neonate (CBL: 19.4 cm) and adult *Pontoporia* (CBL: 38.7 cm) showing the skull and the lower jaw (transparent white), each mandibular fat body (yellow) and the tympano-periotic complex (dense white). In both views, the tympano-periotic complex shows close topographical relationships to the mandibular fat bodies and the lower jaw. The dotted lines in C and D represent the transverse plane that horizontally crosses the anterior insertion of the nasal bones (see Results).

view of each lower jaw ramus is convex, and the ventral process formed by the posterior end of the mandibular symphysis is projected ventrally (Fig. 3C, 8C). This process passes ventrally through the level between the angle of the mandible and the rostrum anterior tip (n = 23, CBL range: 22.31–33.89 cm). During postnatal development, however, the mandible apparently changes its curvature when it grows distally, and its ventral profile turns from convex into concave. This feature is characterized by the ventral process surpassing the level that passes between the angular process and the mandibular tip (n = 46, CBL range: 27.68–42.27 cm) (Fig. 3D, 8D).

The dental alveoli of the lower jaw mark the site where the teeth are formed and develop from posterior to anterior in the tooth row. Here, a series of interalveolar septa begins to develop on both sides of the alveolar border by small projections that join each other to form the dental alveoli (Fig. 9). Accordingly, the fully developed dental alveoli are characterized by a complete closure of interalveolar septa. In our osteological data, it was found that only one smaller specimen had no projections of interalveolar septa (CBL: 23.00 cm). In general, there is a considerable variability in *Pontoporia*'s tooth row development with regard to skull size. Seven individuals exhibited only one formed dental alveolus (CBL range: 30.13–33.80 cm). Nine individuals exhibited formed dental alveoli surpassing the caudal half of the alveolar groove (CBL range: 27.59–40.97 cm). All dental alveolar septa were well formed in 13 individuals (CBL range: 36.23–42.27 cm). In general, it was shown that this developmental feature did not clearly correlate to skull size.

The mandibular fat bodies (Mfb), situated within the mandible foramen and directly lateral to the acoustic window, show an anterior elongation, more noticeable

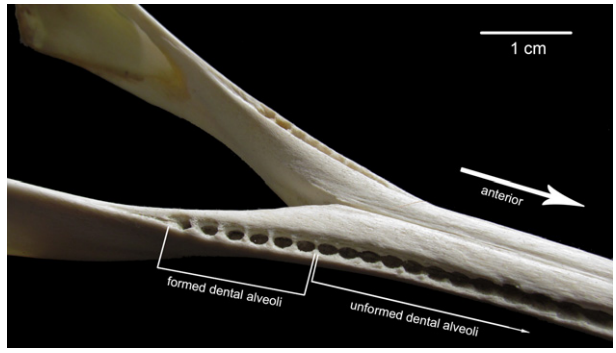

Figure 9. Diagonal dorsal view of subadult mandibular bone of *Pontoporia* showing six closed (formed) dental alveoli. Anteriorly, the level of alveolus closure decreases progressively. GEMARS 1403, CBL: 38.36 cm.

in adults than in neonates (Fig. 8). The differences between the axial lengths of both Mfb in the neonate (right 61.03 mm; left 55.45 mm) and the adult (right 121.1 mm, left 117.61 mm) specimens represent this anterior elongation when we compare it to their width (neonate's right 10.66 mm, left 12.19 mm; adult's right 15.51 mm, left 14.39 mm). This means that the Mfb axial length in relation to its CBL in the adult is approximately 1.3 times longer when compared to the neonates. In addition, a decrease in mean (HU) density was observed in the adult Mfb (right –92.40 HU SD: 28.70, left –80.36 HU SD: 23.68) when compared to the neonate (right –59.51 HU SD: 23.69, left –60.45 HU SD: 22.95). A thin external mandibular fat body first described by Norris (1968) was dissected in neonate and adult specimens, but not reconstructed from the CT images.

Tympano-periotic complex—After birth, there is a decrease in the tympano-periotic complex size relative to the skull length (CBL) in which the standard length of the tympanic bone represents ~10.5% in the neonate specimen and ~5.6% in the adult (Fig. 8). The same situation was found for the tympanic bone width (neonate: ~7.1%, adult: ~3.6%), periotic length (neonate: ~10.2%,; adult: ~6%), and periotic width (neonate: ~8%, adult: ~4.2%). As to volume values, the neonate tympano-periotic complex (right 2,477.19 mm^3, left 2,436.73 mm^3) corresponded to more than 70% of the volume of the adult structure (right 3,242.68 mm^3, left 3,447.99 mm^3). These data demonstrate that the tympano-periotic complex showed fewer modifications during postnatal development than all other biosonar relevant structures analyzed here.

Discussion

Topographical changes of *Pontoporia*'s sound generating apparatus throughout postnatal ontogeny shown here may functionally represent a change of sound production and emission capabilities. McKenna *et al.* (2012) suggested that odontocete biosonar capabilities are directly related to the melon shape. In addition, the connective tissue around the melon affects sound emission and the rostral muscles may act on the melon shape for sound adjustments (Mead 1975, Harper *et al.* 2008). The

trumpet form of the posterior part of the right branch of the melon in *Pontoporia* may be modulated by its related muscles to control the sound beam resulting in an elongated lens for conducting and frequency filtering the pulses generated at the MLDB complex. The presence of rostral musculature in neonate specimens may represent an additional system to adjust the sound beam and would suggest that special motor skills can be learned by neonates. In contrast, adult specimens should have a less mobile melon due to the lack of rostral muscles and have, thus, less possibilities to modulate the sound beam by the melon. On the other hand, the left branch of melon reveals similar shape in young and adult specimens and can represent the constant mechanism of sound emission in their life-stories. Accordingly, each fatty pathway should correspond to a distinct sound transmission pathway and should be functionally different from its counterpart.

It was shown that the nasal air sacs of a dolphin's head may function as acoustic reflectors in echolocation and sound beam formation (Mead 1975, Aroyan *et al.* 1992, Cranford *et al.* 1996). These air spaces are extremely variable, both within a single species and between odontocete species (Mead 1975, Dormer 1979, Cranford *et al.* 1996, Huggenberger *et al.* 2008). The dense tissue around the nasofrontal sacs may be similar to the porpoise capsule first described by Cranford *et al.* (1996). Moreover, this dense tissue may be crucial for the generation of *Pontoporia*'s narrow-band high-frequency clicks (Melcón *et al.* 2012) because Huggenberger *et al.* (2009) has hypothesized that the dense and stiff porpoise capsule is one of the prerequisites for the production of such narrow-band, high-frequency signals in *Phocoena phocoena* due to its stiffness. Also, the trabeculae of the intrinsic musculature in the nasofrontal air sacs have not been described before for *Pontoporia*. Mead (1975) found a similar situation for *Globicephala* that may allow a partial compression of this air sac. The hyperdeveloped right vestibular air sac (VS) is thought to reflect and guide the sound generated at the right MLDB complex (Cranford *et al.* 1996, Huggenberger *et al.* 2010). The less developed neonate's VS do not cover the dorsal melon surface as it does in adults. Accordingly, the VS may be more effective to concentrate and "trap" the sound energy within the melon pathway.

Another river dolphin, *Platanista gangetica* (Odontoceti: Platanistidae), does not exhibit vestibular air sacs, although its maxillary crests can reveal a functional convergence (Pilleri 1979). In this species, the ascendant part of maxilla develops dorsally above the epicranial complex and accompanies an extensive air sinus which does not communicate with the nasal cavity, but with the periotic sinus and tympanic cavity (Pilleri 1979). In contrast to other odontocetes, these superficial air sacs covering the nasal complex dorsally may be controlled independently from the air pressure in the nasal tracts of *Platanista*.

Odontocete mandibles serve a variety of functions, mainly feeding and hearing (Barroso *et al*. 2012). Today's most discussed hypothesis for the sound perception pathway was proposed by Norris (1968) according to which the sound, that enters the lower jaw of odontocetes closely to the posterior part of the alveolar process, is transmitted *via* the mandibular pan bone (acoustic window) and then guided by the medial mandibular fat pad through an extended mandibular foramen to the tympanic bulla. Bullock *et al.* (1968) and McCormick *et al.* (1970) demonstrated that dolphins are highly sensitive to sound at the tip of the lower jaw up to areas below the eye.

Although routine modern imaging techniques are unable to detect delicate structures in the tympano-periotic complex and the ear ossicles (malleus, incus, and stapes) (Ketten 1994, Gutstein *et al.* 2014) it is remarkable that the neonate ear complex volume and anatomy matches the adult shape and volume more than the rest of the

head. Recent findings demonstrate that newborn bottlenose dolphins are capable of whistle learning (Killebrew *et al.* 2001, Morisaka *et al.* 2005, Favaro *et al.* 2013), and that the first pulse trains can be recorded on the 14th day of life (Favaro *et al.* 2013). Our anatomical data suggest that the sound generating system and the auditory sense may be functional at birth, since the location of the mandibular fat bodies relative to the mandible foramen in the neonates supports the function proposed by Norris (1968). Although the vocal learning capabilities of newborn *Pontoporia* are still unknown, the fact that the shape and the properties (density) of the mandibular fat pad differ between neonates and adults points out that the characteristics of the receiving apparatus for echolocation signals in neonates should differ from the adult's situation. The mechanism of sound transmission is not understood in detail since both structures (fat body and tympanic bulla), adjacent to each other, are characterized by a high impedance mismatch. However, in a recent paper using finite elements methods, Cranford *et al.* (2010) showed that the ear ossicles may be sensitive to complex high-frequency vibrations of the tympanic bulla evoked by vibrations across the large contact area with the mandibular fat body.

Their small size and the "countershaded" coloration (Trimble and Praderi 2006), along with their rare aerial displays, make it difficult to study *Pontoporia* in the wild (Bordino *et al.* 1999, Melcón *et al.* 2012). Trophic studies of this species indicate, at least, 76 prey types including mainly fish (~80%), crustaceans (~9%), and molluscs (~8%) (Danilewicz *et al.* 2002). However, older animals show greater variability of food items compared to weaned calves (Rodríguez *et al.* 2002). This change in diet through their ontogeny reveals an estuarine dependence for young individuals on shrimp. The first predation activities in *Pontoporia* start at a young age (2.5–3 mo) when they are approximately 75 cm long, and the animals tend to feed independently from the mother's milk at the age of 7 mo, when they reach a length of approximately 95 cm (Danilewicz *et al.* 2002). Riccialdelli *et al.* (2013) have presented a "diet shift hypothesis" suggesting that the ontogenetic diet shift in Commerson's dolphins (*Cephalorhynchus commersonii*) may be related to the improvement of foraging skills and the expansion of habitats by older animals, as well as the increase in diving capabilities. However, such a correlation between behavior and feeding has not been reported so far for *Pontoporia*.

The postnatal ontogenetic changes observed in the biosonar relevant structures in *Pontoporia* correlate in time with its ontogenetic diet shift. The fact that slow moving shrimp are the most important diet component in the first predation activities of *Pontoporia* may be related to limitations of general motor skills as well as of the echolocation system of young individuals. Gardner *et al.* (2007) have pointed out that the echolocation capabilities in odontocetes are not inherited, but developed in a combination of the physiological maturation and learning behaviors. The ontogenetic changes observed in the main biosonar structures in *Pontoporia* demonstrate an early but continuing postnatal maturation of the echolocation system. Tellechea and Norbis (2014) have recently reported that neonatal *Pontoporia* dolphins are active acoustically at 1 wk old. They can produce high frequency clicks (PFA, peak frequency average: 80 KHz, CD, click duration: 0.20 ms), low frequency clicks (PFA: 12.52 KHz, CD: 0.22 ms), and burst clicks (PFA: 47.44 KHz, CD: 13 ms). These burst clicks emitted by neonatal *Pontoporia* dolphins resemble the communication clicks in *Phocoena phocoena* (Clausen *et al.* 2011) and could be important for *Pontoporia*'s mother-calf communication (Tellechea and Norbis 2014). Also, the latter authors have pointed out that the increase of click duration and frequencies reported for

adults (PFA: 149 KHz, CD: 5 s) (Melcón *et al.* 2012) may be due to immaturely developed acoustic and neuromuscular skills (Tellechea and Norbis 2014).

Although one must be careful with functional interpretations of anatomical findings (Cranford *et al.* 1996, McKenna *et al.* 2012), we hypothesize that the peculiar development of the main biosonar structures described in this study may be one cause among others for the increased bycatch mortality and the diet shift of young *Pontoporia*. Due to improved motor skills and probably more experience adult *Pontoporia* are also less threatened by incidental catches and more successful in catching different types of prey because of improved echolocation skills.

Acknowledgments

This study was made possible through the cooperation and friendship of fishermen from Tramandaí, Imbé, and Torres, Brazil. We are thankful to the Study Group of Aquatic Mammals of Rio Grande do Sul (Grupo de Estudos de Mamíferos Aquáticos do Rio Grande do Sul-GEMARS) for collection of and access to the franciscana's skull. Many thanks to Dr. S. Siciliano and Msc. R. Machado for logistics support, and to the Department de Zoology (IB/UFRGS) and Center for Coastal, Limnological and Marine Studies (Centro de Estudos Costeiros, Limnológicos e Marinhos - CECLIMAR/IB/UFRGS) for technical assistance. Thanks to M. Bemvenuti and Clínicas SIDI for making it possible to perform the CT and MRI scans. We are grateful to Dr. L. R. Malabarba, Dr. D. Rodríguez, Dr. N. Pyenson, Dr. S. Thornton, Dr. F. Fish, Dr. D. Boness, and two other anonymous reviewers for their suggestions and comments. Thanks to Liege Frainer Barbosa for proofreading the manuscript in English. This paper is part of first author's M.Sc. studies, funded by CAPES (2011 to 2013).

Literature Cited

Akamatsu, T., J. Teilmann, L. A. Miller, *et al.* 2007. Comparison of echolocation behaviour between coastal and riverine porpoises. Deep Sea Research Part II: Topical Studies in Oceanography 54:290–297.

Aroyan, J. L. 2001. Three-dimensional modeling of hearing in *Delphinus delphis*. The Journal of the Acoustical Society of America 110:3305–3318.

Aroyan, J. L., T. W. Cranford, J. Kent and K. S. Norris. 1992. Computer modeling of acoustic beam formation in *Delphinus delphis*. The Journal of the Acoustical Society of America 92:2539–2545.

Barnes, L. G. 1985. Fossil pontoporiid dolphins (Mammalia: Cetacea) from the Pacific coast of North America. Contributions in Science, Natural History Museum of Los Angeles County 363:1–34.

Barroso, C., T. W. Cranford and A. Berta. 2012. Shape analysis of odontocete mandibles: Functional and evolutionary implications. Journal of Morphology 273:1021–1030.

Bordino, P., G. Thompson and M. Iñíguez. 1999. Ecology and behaviour of the franciscana (*Pontoporia blainvillei*) in Bahía Anegada, Argentina. Journal of Cetacean Research and Management 1:213–222.

Bordino, P., S. D. Kraus, D. Albareda, *et al.* 2002. Reducing incidental mortality of franciscana dolphin *Pontoporia blainvillei* with acoustic warning devices attached to fishing nets. Marine Mammal Science 18:833–842.

Bordino, P., A. I. Mackay, T. B. Werner, S. P. Northridge and A. J. Read. 2013. Franciscana bycatch is not reduced by acoustically reflective or physically stiffened gillnets. Endangered Species Research 21:1–12.

Bullock, T., A. Grinnell, E. Ikezono, *et al.* 1968. Electrophysiological studies of central auditory mechanisms in cetaceans. Journal of Comparative Physiology A: Neuroethology, Sensory, Neural, and Behavioral Physiology 59:117–156.

Burmeister, G. 1867. Descripcion de cuatro especies de Delfinides de la costa Argentina en el Oceano Atlantico [Description of four delphinid species from the Argentine coast in the Atlantic Ocean]. Annales de Museo Publico de Buenos Aires 1:367–445.

Clausen, K. T., M. Wahlberg, K. Beedholm, S. Deruiter and P. T. Madsen. 2011. Click communication in harbour porpoises *Phocoena phocoena*. Bioacoustics 20:1–28.

Cranford, T. W., M. Amundin and K. S. Norris. 1996. Functional morphology and homology in the odontocete nasal complex: Implications for sound generation. Journal of Morphology 228:223–285.

Cranford, T. W., and M. Amundin. 2004. Biosonar pulse production in odontocetes: The state of our knowledge. Pages 27–35 *in* J. A. Thomas, C. F. Moss and M. Vater, eds. Echolocation in bats and dolphins. The University of Chicago Press, Chicago, IL.

Cranford, T. W., P. Krysl and J. A. Hildebrand. 2008*a*. Acoustic pathways revealed: Simulated sound transmission and reception in Cuvier's beaked whale (*Ziphius cavirostris*). Bioinspiration & Biomimetics 3:1–10.

Cranford, T. W., M. F. Mckenna, M. S. Soldevilla, *et al.* 2008*b*. Anatomic geometry of sound transmission and reception in Cuvier's beaked whale (*Ziphius cavirostris*). The Anatomical Record 291:353–378.

Cranford, T. W., P. Krysl and M. Amundin. 2010. A new acoustic portal into the odontocete ear and vibrational analysis of the tympanoperiotic complex. PLOS ONE 5 (8):e11927.

Danilewicz, D., F. Rosas, R. Bastida, J. Marigo, M. Muelbert and D. Rodríguez. 2002. Report of the working group on biology and ecology. Latin American Journal of Aquatic Mammals 1:25–42.

De Moraes, T. F., P. H. J. Amorim, F. Azevedo, *et al.* 2012. InVesalius—An open-source imaging application. World Journal of Urology 30:687–691.

Dormer, K. J. 1979. Mechanism of sound production and air recycling in delphinids: Cineradiographic evidence. The Journal of the Acoustical Society of America 65:229–239.

Evans, W. E. and J. H. Prescott. 1962. Observations of sound production capabilities of the bottlenose porpoise: A study of whistles and clicks. Zoologica 47:121–128.

Favaro, L., G. Gnone and D. Pessani. 2013. Postnatal development of echolocation abilities in a bottlenose dolphin (*Tursiops truncatus*): Temporal organization. Zoo Biology 32:210–215.

Fraser, F. C., and P. E. Purves. 1960. Hearing in cetaceans. Bulletin of the British Museum (Natural History) 7:1–140.

Galatius, A., A. Berta, M. S. Frandsen and R. N. P. Goodall. 2011. Interspecific variation of ontogeny and skull shape among porpoises (Phocoenidae). Journal of Morphology 272:136–148.

Gardner, S., G. Ylitalo and U. Varanasi. 2007. Comparative assessment of organochlorine concentrations in porpoise melon and blubber. Marine Mammal Science 23:434–444.

Geraci, J. R., and V. J. Lounsbury. 1993. Marine mammals ashore: A field guide for strandings. Sea Grant College Program, Texas A&M University, College Station, TX.

Gutstein, C. S., C. P. Figueroa-Bravo, N. D. Pyenson, R. E. Yury-Yañez, M. A. Cozzuol and M. Canals. 2014. High frequency echolocation, ear morphology, and the marine-freshwater transition: A comparative study of extant and extinct toothed whales. Palaeogeography, Palaeoclimatology, Palaeoecology 400:62–74.

Haddad, D., S. Huggenberger, M. Haas-Rioth, L. S. Kossatz, H. H. A. Oelschläger and A. Haase. 2012. Magnetic resonance microscopy of prenatal dolphins (Mammalia, Odontoceti, Delphinidae)—ontogenetic and phylogenetic implications. Zoologischer Anzeiger 251:115–130.

Harper, C., W. Mclellan, S. Rommel, D. Gay, R. Dillaman and D. Pabst. 2008. Morphology of the melon and its tendinous connections to the facial muscles in bottlenose dolphins (*Tursiops truncatus*). Journal of Morphology 269:820–839.

Huggenberger, S. M. A., M. A. Rauschmann and H. H. A. Oelschläger. 2008. Functional morphology of the hyolaryngeal complex of the harbor porpoise (*Phocoena phocoena*): Implications for its role in sound production and respiration. The Anatomical Record 291:1262–1270.

Huggenberger, S., M. A. Rauschmann, T. J. Vogl and H. H. A. Oelschläger. 2009. Functional morphology of the nasal complex in the harbour porpoise (*Phocoena phocoena* L.). The Anatomical Record 292:902–920.

Huggenberger, S., T. J. Vogl and H. H. A. Oelschläger. 2010. Epicranial complex of the La Plata dolphin (*Pontoporia blainvillei*): Topographical and functional implications. Marine Mammal Science 26:471–481.

Kasuya, T. 1973. Systematic consideration of recent toothed whales based on the morphology of tympano-periotic bone. Scientific Reports of the Whales Research Institute, Tokyo 25:1–103.

Ketten, D. R. 1994. Functional analyses of whale ears: Adaptations for underwater hearing. Oceans Engineering for Today's Technology and Tomorrow's Preservation 1:264–270.

Killebrew, D. A., E. I. Mercado, L. M. Herman and A. A. Pack. 2001. Sound production of a neonate bottlenose dolphin. Aquatic Mammals 27:34–44.

Kraus, S. D., S. J. Read, A. Solow, *et al.* 1997. Acoustic alarms reduce porpoise mortality. Nature 388:525.

Manger, P. R. 2006. An examination of cetacean brain structure with a novel hypothesis correlating thermogenesis to the evolution of a big brain. Biological Reviews 81:293–338.

McCormick, J. G., E. G. Wever, J. Palin and S. H. Ridgway. 1970. Sound conduction in the dolphin ear. The Journal of the Acoustical Society of America 48:1418–1428.

McKenna, M. F., J. A. Goldbogen, J. St Leger, J. A. Hildebrand and T. W. Cranford. 2007. Evaluation of postmortem changes in tissue structure in the bottlenose dolphin (*Tursiops truncatus*). The Anatomical Record 290:1023–1032.

McKenna, M. F., T. W. Cranford, A. Berta and N. D. Pyenson. 2012. Morphology of the odontocete melon and its implications for acoustic function. Marine Mammal Science 28:690–713.

Mead, J. G. 1975. Anatomy of the external nasal passages and facial complex in the Delphinidae (Mammalia: Cetacea). Smithsonian Contributions to Zoology 207:1–35.

Mead, J., and R. Fordyce. 2009. The therian skull: A lexicon with emphasis on the odontocetes. Smithsonian Contributions to Zoology:1–248.

Melcón, M. L., M. Failla and M. A. Iñíguez. 2012. Echolocation behavior of franciscana dolphins (*Pontoporia blainvillei*) in the wild. The Journal of the Acoustical Society of America 131:448–453.

Moran, M. M., S. Nummela and J. Thewissen. 2011. Development of the skull of the pantropical spotted dolphin (*Stenella attenuata*). The Anatomical Record 294:1743–1756.

Moreno, I. B., P. H. Ott and D. Danilewicz. 1997. Análise preliminar do impacto da pesca artesanal costeira sobre Pontoporia blainvillei no litoral norte do Rio Grande do Sul, sul do Brasil [Preliminary impact analysis of coastal artesanal fisheries on Pontoporia blainvillei in the north coast of Rio Grande do Sul, southern Brazil]. Pages 31–41 *in* M. C. Pinedo and A. S. Barreto, eds. Anais do 2° Encontro sobre Coordenação de Pesquisa e Manejo da Franciscana. FURG, Rio Grande, Brazil.

Morisaka, T., M. Shinohara and M. Taki. 2005. Underwater sounds produced by neonatal bottlenose dolphins (*Tursiops truncatus*). II. Potential function. Aquatic Mammals 31:258–265.

Ness, A. R. 1967. A measure of asymmetry of the skulls of odontocete whales. Journal of Zoology 153:209–221.

Norris, K. 1968. The evolution of acoustic mechanisms in odontocete cetaceans. Pages 297–324 *in* E. T. Drake, ed. Evolution and environment. Yale University Press, New Haven, CT.

Norris, K. S., and G. W. Harvey. 1974. Sound transmission in the porpoise head. The Journal of the Acoustical Society of America 56:659–664.

Norris, K. S., J. H. Prescott, P. V. Asa-Dorian and P. Perkins. 1961. An experimental demonstration of echo-location behavior in the porpoise, *Tursiops truncatus* (Montagu). Biological Bulletin 120:163–176.

Oelschläger, H. H. A., M. Haas-Rioth, C. Fung, S. H. Ridgway and M. Knauth. 2008. Morphology and evolutionary biology of the dolphin (*Delphinus* sp.) brain—MR imaging and conventional histology. Brain, Behavior and Evolution 71:68–86.

Pilleri, G. 1979. The blind Indus dolphin, *Platanista indi*. Endeavour 3:48–56.

Praderi, R., M. Pinedo and E. Crespo. 1989. Conservation and management of *Pontoporia blainvillei* in Uruguay, Brazil and Argentina. Pages 52–55 *in* W. F. Perrin, R. L. Brownell Jr., Z. Kaiya and L. Jiankang, eds. Biology and conservation of the river dolphins. Occasional Papers of the IUCN, Species Survival Commission 3, Gland, Switzerland.

Prophet, E. B., B. Mills, J. B. Arrington and L. H. Sobin. 1992. Laboratory methods in histotechnology. American Registry of Pathology, Washington, DC.

Purves, P., and G. Pilleri. 1983. Echolocation in whales and dolphins. Academic Press, London, U.K.

Ramos, R. M. A., A. P. M. Di Beneditto and N. R. W. Lima. 2000. Growth parameters of *Pontoporia blainvillei* and *Sotalia fluviatilis* (Cetacea) in northern Rio de Janeiro, Brazil. Aquatic Mammals 26:65–75.

Rauschmann, M. A., S. Huggenberger, L. S. Kossatz and H. H. A. Oelschläger. 2006. Head morphology in perinatal dolphins: A window into phylogeny and ontogeny. Journal of Morphology 267:1295–1315.

Read, A. J., D. M. Waples, K. W. Urian and D. Swanner. 2003. Fine-scale behaviour of bottlenose dolphins around gilnets. Proceedings of the Royal Society of London B 270: S90–S92.

Riccialdelli, L., S. D. Newsome, N. A. Dellabianca, R. Bastida, M. L. Fogel and R. N. P. Goodall. 2013. Ontogenetic diet shift in Commerson's dolphin (*Cephalorhynchus commersonii commersonii*) off Tierra del Fuego. Polar Biology 36:617–627.

Robb, R. A. 1999. Biomedical imaging, visualization, and analysis. John Wiley & Sons Inc, New York, NY.

Rodríguez, D., L. Rivero and R. Bastida. 2002. Feeding ecology of the franciscana (*Pontoporia blainvillei*) in marine and estuarine waters of Argentina. Latin American Journal of Aquatic Mammals 1:77–94.

Schenkkan, E. 1972. On the nasal tract complex of *Pontoporia blainvillei* Gervais and d'Orbigny 1844 (Cetacea, Platanistidae). Investigations on Cetacea 4:83–90.

Schwerdtfeger, W. K., H. H. A. Oelschläger and H. Stephan. 1984. Quantitative neuroanatomy of the brain of the La Plata dolphin, *Pontoporia blainvillei*. Anatomy and Embryology 170:11–19.

Secchi, E. R., A. N. Zerbini, M. Bassoi, L. Dalla-Rosa, L. M. Moller and C. C. Rocha-Campos. 1997. Mortality of franciscanas, *Pontoporia blainvillei*, in coastal gillnetting in southern Brazil: 1994–1995. Report of the International Whaling Commission 47:653–658.

Secchi, E. R., P. Ott, E. Crespo, P. G. Kinas, S. Pedraza and P. Bordino. 2001. A first estimate of franciscana (*Pontoporia blainvillei*) abundance off southern Brazil. Journal of Cetacean Research and Management 3:95–100.

Secchi, E. R., D. Danilewicz and H. Ott. 2003. Applying the phylogeographic concept to identify franciscana dolphin stocks: Implications to meet management objectives. The Journal of Cetacean Research and Management 5:61–68.

Tellechea, J. S., and W. Norbis. 2014. Sound characteristics of two neonatal franciscana dolphins (*Pontoporia blainvillei*). Marine Mammal Science 30:1573–1580.

Trimble, M., and R. Praderi. 2006. What is the colour of the franciscana (*Pontoporia blainvillei*)? A review and a proposed assessment method. Latin American Journal of Aquatic Mammals 5:55–63.

Received: 7 August 2014
Accepted: 16 December 2014